EPJ Web of Conferences **45**, 01069 (2013)
DOI: 10.1051/epjconf/20134501069

Laser-optical and numerical Research of the flow inside the lubricating gap of a journal bearing model

M. Nobis[1], P. Stücke[1], M. Schmidt[1], and M. Riedel[1]

[1]West Saxon University of Applied Sciences Zwickau, Dr.Friedrichs Ring 2a, 08056 Zwickau,

Abstract. The laser-optical research of the flow inside the lubricating gap of a journal bearing model is one important task in a larger overall project. The long-term objective is the development of an easy-to-work calculation tool which delivers information about the causes and consequences of cavitation processes in hydrodynamically lubricated journal bearings. Hence, it will be possible to find statements for advantageous and disadvantageous geometrical shapes of the bushings. In conclusion such a calculation tool can provide important insights for the construction and design of future journal bearings. Current design programs are based on a two-dimensional approach for the lubricating gap. The first dimension is the breath of the bearing and the second dimension is the circumferential direction of the bearing. The third dimension, the expansion of the gap in radial direction, will be neglected. Instead of an exact resolution of the flow pattern inside the gap, turbulence models are in use. Past studies on numerical and experimental field have shown that inside the lubricating gap clearly organized and predominantly laminar flow structures can be found. Thus, for a detailed analysis of the reasons and effects of cavitation bubbles, a three-dimensional resolution of the lubricating gap is inevitable. In addition to the qualitative evaluation of the flow with visualization experiments it is possible to perform angle-based velocity measurements inside the gap with the help of a triggered Laser-Doppler-Velocimeter (LDV). The results of these measurements are used to validate three-dimensional CFD flow simulations, and to optimize the numerical mesh structure and the boundary conditions. This paper will present the experimental setup of the bearing model, some exemplary results of the visualization experiments and LDV measurements as well as a comparison between experimental and numerical results..

1 Introduction

In the small gap between the rotating shaft and the stationary bushing of a hydrodynamically lubricated journal bearing three-dimensional flow structures can be found. The properties of this flow depend on the rotational speed, the geometrical features, and the incoming and outgoing mass flows. The feedhole for the incoming mass flow and the axial bearing ends respectively the hole in the rotating shaft for the partial outgoing mass flows define the boundaries of the system. In 1995 *Wollfarth* [1] investigated experimentally the erosion in journal bearings caused by cavitation. In this work the parameters supplied mass flow rate, Reynolds number and the load of the bearing were varied. Moreover, different configurations of shaft and bushing were combined. For many of all configurations no cavitation could be generated. Only in a few cases cavitation could be produced repeatable. The base for the results which are shown in this present paper gives a journal bearing which tended to reproducible cavitation.

The original mounting place of this journal bearing was a middle position of the crankshaft main bearings in the diesel engine of a truck.

In this specific case of a crankshaft main bearing of multi-cylinder engines there is a circumferential groove over 180° in the bushing into which the feedhole enters. The groove distributes the fresh oil and transmits the oil in combination with the hole in the crankshaft to the bearings of the connecting rod (see figure 1). Caused by the continuously changing position of the hole in the shaft in opposite to the feedhole in the bushing a transient or respectively a periodic flow over 360° results.

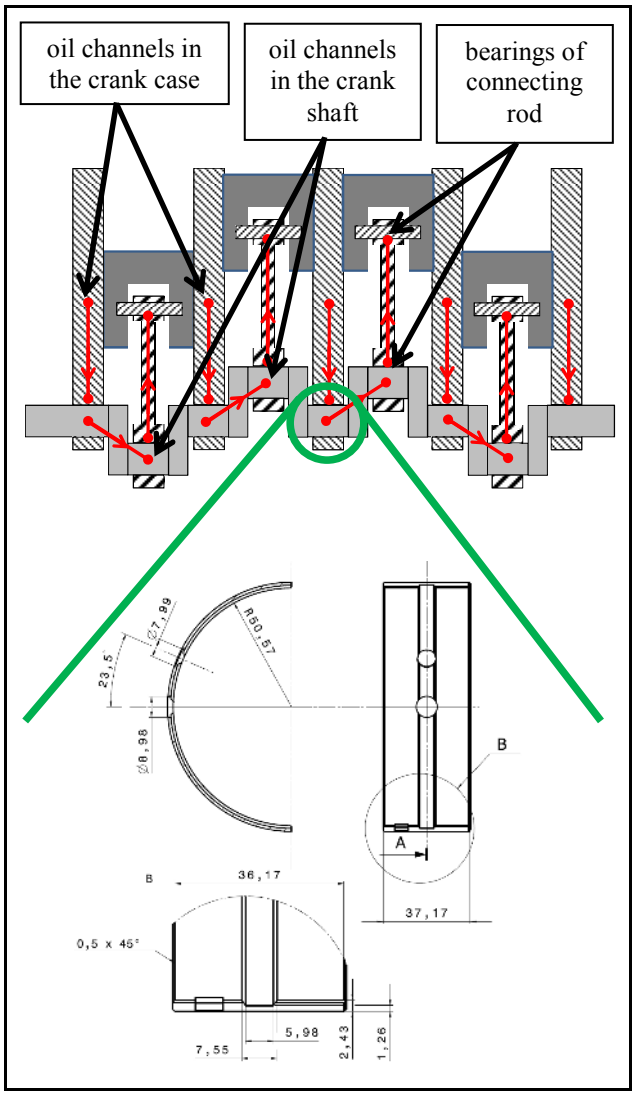

Fig. 1: crankshaft main bearings in a four-cylinder engine

2 Geometrical parameters

Figure 2 shows schematically a longitudinal and a cross-section through the bearing model. Such a simplified system can be described by a fixed outer and a rotating inner cylinder. Like in a real journal bearing there may be an eccentricity between the rotating shaft and the bushing. This eccentricity is given by the displacement e between the two cylinders. In addition to the main geometric parameters of the system, the basic mass flows Q_{in}, Q_0 and Q_{out} are illustrated.

In the equations 1 to 8 characteristic parameters are defined. The typical Reynolds number range for automotive applications is between 10 and 40.

$$H_0 = R_2 - R_1 \tag{1}$$

$$\Psi = \frac{H_0}{R_1} \tag{2}$$

$$\Gamma = \frac{B}{H_0} \tag{3}$$

$$U_1 = \omega \cdot R_1 \tag{4}$$

$$Re = \frac{H_0 \cdot R_1 \cdot \omega}{\upsilon} \tag{5}$$

$$\varepsilon = \frac{e}{H_0} \tag{6}$$

$$Q_0 = 0{,}5 \cdot B \cdot H_0 \cdot U_1 \tag{7}$$

$$\alpha = \frac{Q_{in}}{Q_0} \tag{8}$$

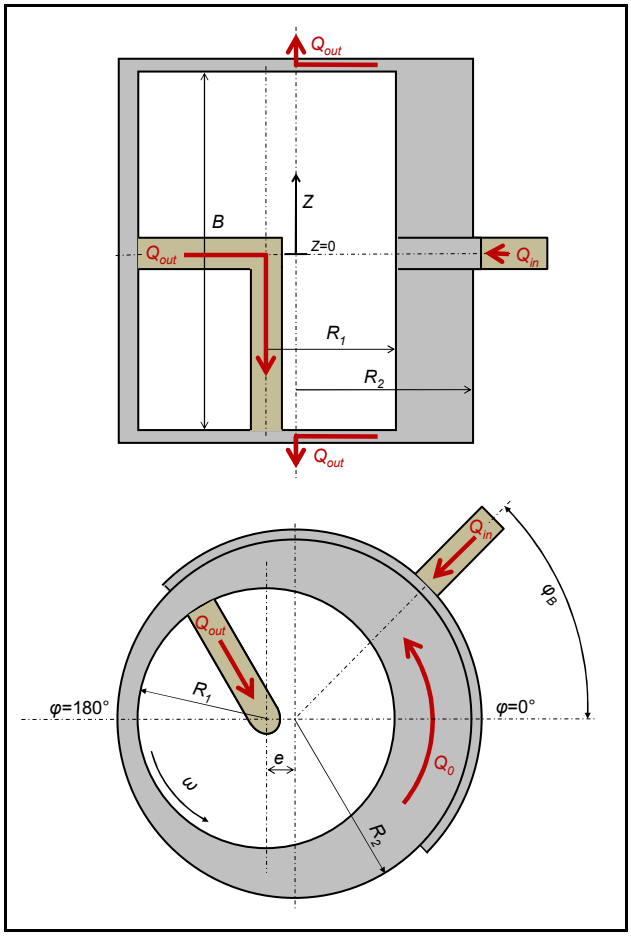

Fig. 2: Geometrical parameters

3 Experimental setup

The design and manufacture of the journal bearing model test rig is based on the geometrical shapes of the bushing shown in figure 1. The groove is simplified to a rectangular profile without any bevels. Further, the notch for fixing the bushing in the crankcase against rotation is neglected. All other geometrical parameters were transferred from the real bearing to the test rig with a scale of 1:3.

A significant difference between the test rig and a real journal bearing is the relative gap width. The Test rig has a relative gap width of $\psi \approx 2.5\,\%$. However a real journal bearing has a relative gap width about $\psi \approx 0.1\,\%$. Increasing the gap width at the test rig is absolutely necessary in order to provide a sufficient optical access to the LDV. To ensure nevertheless the similarity of the flow, the Reynolds number is set like in a real journal bearing. The stationary outer cylinder is

made of acrylic glass and equipped with the feed hole and circumferential groove. It can be positioned as required in an eccentric position with respect to the inner cylinder (see figure 2). For adjusting the eccentricity there are radially mounted measuring screws (see figure 3). The outer cylinder is fixed on a rotary table with the help of clamping claws. Caused by the attachment on a rotary table, it is possible to perform velocity measurements at different angular positions without traversing the LDV in a circular path. The LDV is mounted on an X-Y-traverse system and can be positioned with a high accuracy over the gap by using a coordinates input. The rotating inner cylinder is also made of acrylic glass and is fitted with a radial hole. In addition to the axial outlets this hole defines the third outlet for the supplied mass flow.

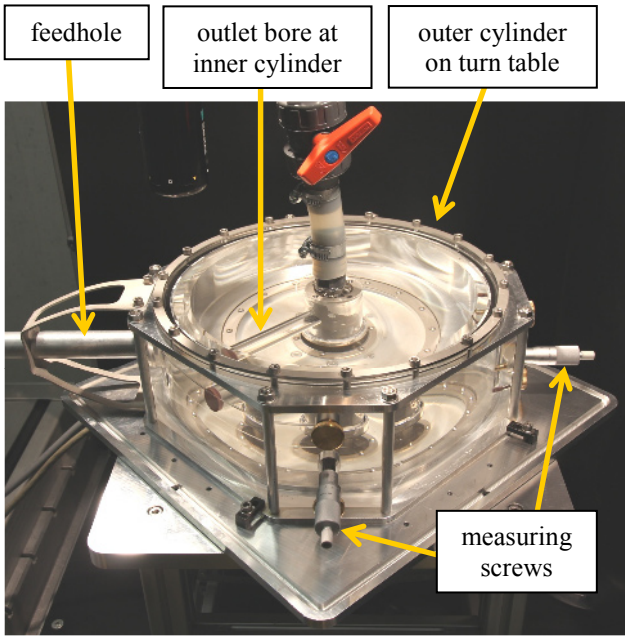

Fig. 3: Bearing modeltest rig in isometric view

For an exact adjustment of the inflowing and outflowing mass flow rates the bearing model is implemented in a hydraulic circuit (see figure 4). This circuit consists of a storage tank, an adjustable oil pump, control valves and three ultrasonic flow meters. The first flow meter measures the supplied volumetric flow rate. The second flow meter is used to control the symmetrical outflow at the axial bearing ends. The amount of oil that flows through the inner cylinder bore (shaft hole) is indicated by the third flow meter. All control valves are used to adjust the distribution of the supplied oil to the individual outlets.

The centrally arranged main shaft with the mounted inner cylinder is driven by a stepping motor. Caused by the design of the actuator with a stepping motor and a toothed drive belt, slip is prevented and it is not necessary to have a permanent real-time monitoring of the rotational speed.

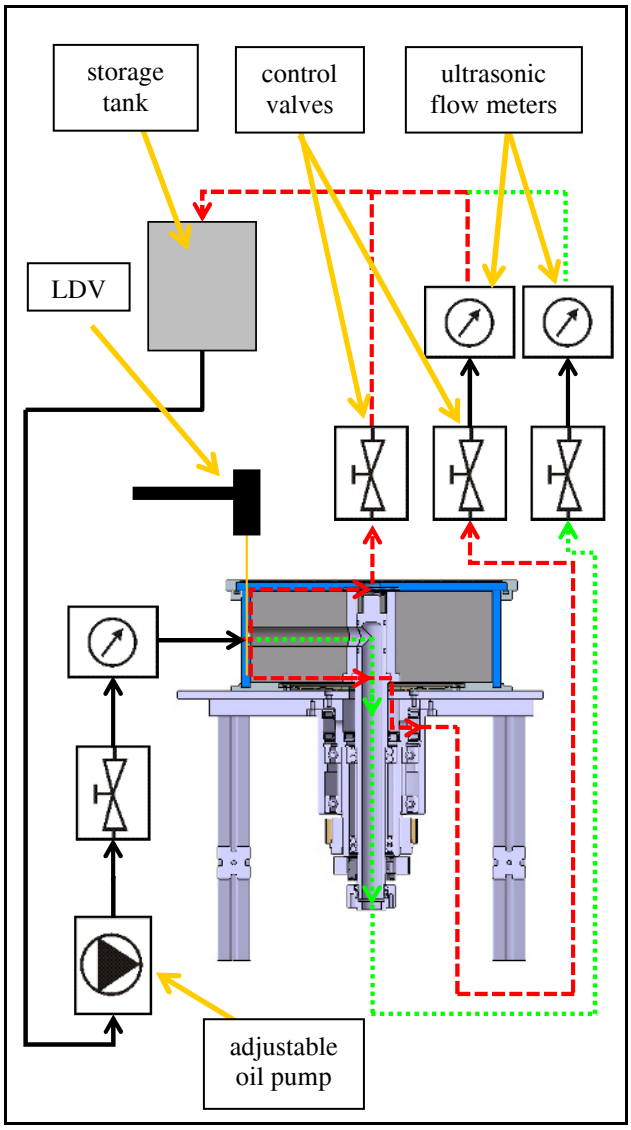

Fig. 4: Hydraulic circuit

4 Results of experimental and numerical researches

The three-dimensional CFD simulations are performed using the software package OpenFOAM. For the presented researches the finite volume method is used. The solution algorithm solves the Navier-Stokes equations and the continuity equation under the specification of laminar flow conditions. To develop a reliably functioning volume mesh and well-fitted boundary conditions a simplified case of the flow in journal bearings is considered at first. For the basic agreement between the experiment and the numerical calculation, it is necessary to investigate the rotating system without incoming and outgoing mass flow rates.

In 2011 *Nobis et. al* [2] presented results of some preliminary works at rotating systems. It must be distinguished between two cases for the design of the boundary conditions at the axial ends of the bearing. Firstly, the system can be considered as an endless wide bearing, if the pressure compensation over the axial ends is prevented. For this case slip-ring seals at the axial end of the rotating inner cylinder are mounted. The

corresponding numerical boundary condition is the zero gradient boundary condition for the pressure. Secondly, if the pressure compensation over the axial ends is allowed, a remarkable reduction of the pressure maximum and minimum in the lubrication gap results. In consequence the measured velocity profiles have a much lower curvature. This property can be defined for the numerical calculation by setting the ambient pressure at the axial bearing ends as boundary condition.

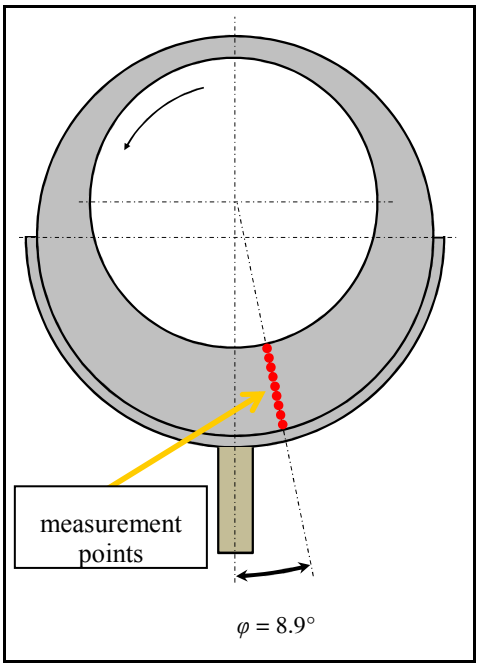

Fig. 5: Measurement points in the gap

For the investigation of these relationships at the current bearing model test rig appropriate measurements and simulations were performed. The schematic cross section in figure 5 illustrates where the individual measurement points are located for determining a velocity profile over the gap width. In axial direction the measurement points are exactly in the middle of the breath B of the System. For all presented results the feedhole is located in the widest gap. Thus, the angular position of the bore is $\varphi_B = 0$ °. Starting from the feed hole the angular position of the measuring points is $\varphi = 8.9$ °. In figure 6 the normalized velocity profiles under the given setting parameters are shown. Due to the adhesion conditions at structures directly at the surface of the inner cylinder the speed is U_1 and at the surface of the outer cylinder the speed is 0.

Due to the high relative eccentricity of $\varepsilon = 90\%$ a back flow region over a wide area of the gap results. The installation of slip-ring seals in the experiment and the specification of a zero gradient boundary condition for the pressure in the numerical simulation provide a good agreement between the results. A correct measurement of velocities directly in the groove requires a high optical surface quality of the groove edges. Currently the data acquisition is done without measurements in the groove and only the velocities in the gap are compared. The laser optical speed measurements directly in the groove are a target in further studies (see section Summary and Outlook).

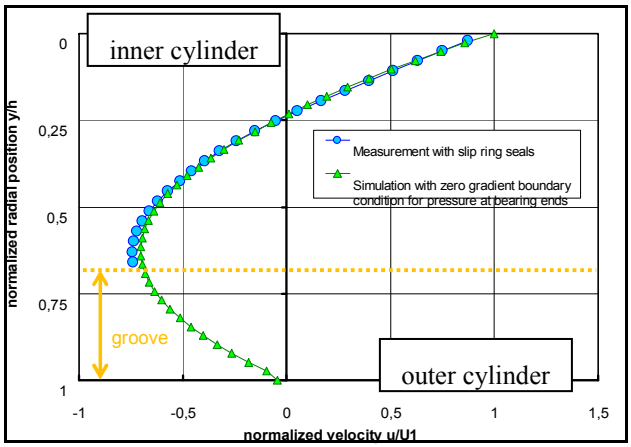

Fig. 6: Comparison of experiment and simulation for $\psi = 2.5$ %, $Re = 65$, $\varepsilon = 90\%$, $\varphi_B = 0°$, $\varphi = 8.9°$, $\alpha = 0\%$

Figure 7 shows the velocity profiles of a LDV measurement and a simulation. In opposite to the chosen parameters of the test case in figure 6 the system is supplied with a mass flow rate Q_{in} in a ratio of $\alpha = 200$ %. The outlets are the upper and lower axial end of the test rig. The oil bore in the inner cylinder is closed. Consequently in the lubrication gap a steady flow does exist. Caused by the additionally applied mass flow rate this tests can only be carried out without slip-ring seals for sealing the axial bearing ends. Thus, the environmental conditions in the lubrication gap change and it is necessary to set a boundary condition for the numerical simulation, which can depict all the attendant effects correctly.

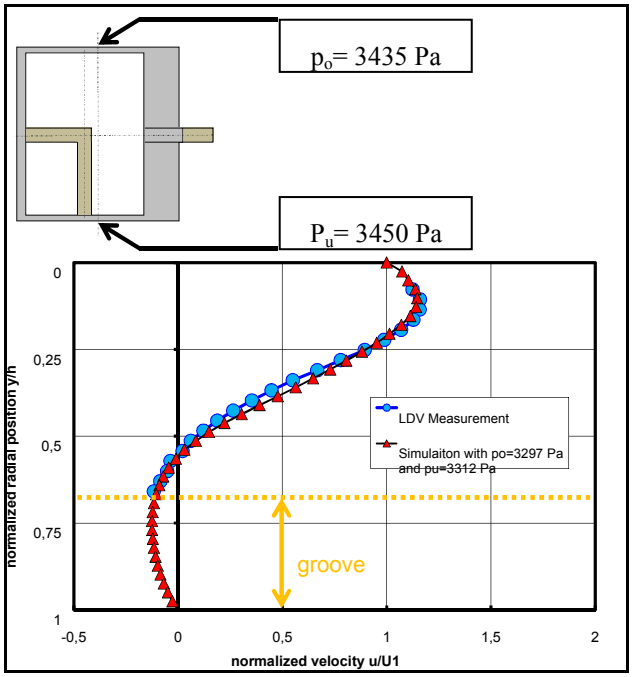

Fig. 7: Comparison of experiment and simulation for $\psi = 2.5$ %, $Re = 65$, $\varepsilon = 90\%$, $\varphi_B = 0°$, $\varphi = 8.9°$, $\alpha = 200\%$ with axial ends as outlets and a fixed pressure at the boundary conditions

For a real journal bearing in the crankcase of a four-stroke engine simplified the ambient pressure can be assumed at the axial bearing end. Transferred to the model test rig this means a pressure-free outflow of the supplied oil via the bearing ends. Hence, for the simulation a pressure boundary condition with the specification of the ambient pressure has to be defined.
Due to the connected hydraulic circuit at the test rig, a pressure-free outflow over the bearing ends is not realizable. The height difference between the storage tank and the bearing model leads to a static pressure at the axial ends. Moreover, if the pump in the circuit is switched on, the pressure loss over the pipes and tubes of the circuit is responsible for an additional increase of the static pressure at the axial bearing ends. In contrast there is a decrease of the static pressure due to the higher velocities. Therefore, in summary there must be defined a pressure for the numerical simulations which is accordingly higher than the ambient pressure. An analytical prediction provides a general indication of the pressure which has to be specified. The static pressure at the bearing ends has a strong influence to the velocity distribution and thus to the global flow structure. For the boundary condition with a relative static pressure of 3435 Pa at the top and a static pressure of 3450 Pa at the bottom there is a good coincidence between the results of the experiment and the simulation.

In figure 8 four measured velocity profiles are presented. Thereby the angular position of the measuring points is again at $\varphi = 8.9°$. Hence, the velocities are measured one bore diameter downstream of the feedhole. The introduced amount of oil is only flowing out via the bore at the rotating inner cylinder. The axial bearing ends are closed and the slip ring seals to eliminate pressure compensation are mounted. Due to the adjusted eccentric position of the outer cylinder and the rotating bore at the inner cylinder there is a constantly changing cross section for the outlet. Therefore, near the groove there is a large cross section and near the smallest gap there is a small cross section for the outlet. The result is a slightly fluctuating flow. The volume flow ratio α is set to an average value of 100%.

As explained in the introduction under these conditions a transient or an over 360° periodic flow results. Consequently, each recorded velocity value needs a corresponding time stamp or a corresponding angular position. For this purpose the test rig is equipped with a light barrier which provides the signal processor of the LDV a reset pulse with each revolution. According to definition an angle of zero degree means a direct alignment of the feedhole in the outer cylinder and the hole for the outgoing mass flow in the inner cylinder (see figure 8 left). The velocities are averaged by an angle of one degree. Hence, at one measuring position in the gap 360 velocity values are generated.

Figure 8 shows an example the velocity profiles for the four inner cylinder positions of 0°, 30°, 60° and 90°. The circumferential rotating hole at the inner cylinder has a significant influence to the velocity distribution in the gap. Especially if the rotating hole is near the measuring point (compare hole at 0° with hole at 30°) there is a big difference between the velocity profiles. If this hole is not directly in vicinity to the measuring position (compare hole at 60° with hole at 90°) the differences between the velocity profiles are significantly smaller. Obviously there are flow conditions in the gap with very small fluctuations over a wide angular range.

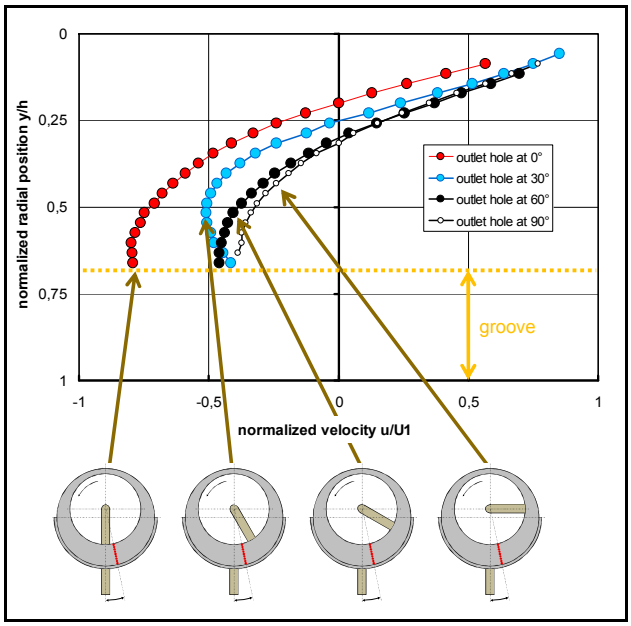

Fig. 8: LDV measurement for $\psi = 2.5$ %, $Re = 65$, $\varepsilon = 90\%$, $\varphi_B = 0°$, $\varphi = 8.9°$, $\alpha = 100\%$ with inner cylinder hole as outlet

However, directly near the hole at the inner cylinder the flow field changes significantly. Visualization experiments show that the outflow via the hole at the inner cylinder brings up a flow reversal at diverse area in the gap. A Back flow area can be converted into a flow with positive rotating direction and conversely a flow area with positive rotating direction can change into a back flow area. Consequently there are flow pattern with large velocity gradients.

5 Summary and Outlook

The investigations have shown that the bearing model test rig is an important tool for the validation of the numerical simulations. The definition of proper boundary conditions and the further development of the volume mesh require repeated comparisons to the reference experiment. Thereby, velocity measurements using an LDV are a very good way to create an experimental database.

In addition to the results which are shown in the article, a parameter variation is provided in which the eccentricity, the Reynolds number and the volumetric flow rates will be variable. The measuring results will be provided to illustrate the relationship of these parameters and will be used repeatedly as a reference for the three-dimensional flow simulation. Moreover, in further investigations velocity measurements will be performed directly in the groove. For this project the surface quality of the groove edges has to be improved to ensure a consistently good reflection of the laser light from the seeding. Moreover, in areas with a large velocity gradient

the fluctuation of the velocity will be captured in order to make statements to the level of turbulence. For the achievement of the long-term objective to apply the numerical simulation with an implemented cavitating model at journal bearing geometries with real gap width ratios, a modification of the bearing model test rig is necessary. The relative gap width has to be downsized. With the knowledge gained to date a reduction of the relative gap width to $\psi \approx 1{,}0$ % should be technically possible. The decrease of the gap width will be realized by an increase of the inner cylinder diameter.

For the considered case with the outflow of the fluid via the inner cylinder bore it is necessary to define a zero gradient pressure boundary condition at the bearing ends for the numerical calculation. With setting the inner cylinder bore to the outlet a new problem results. The volume mesh has to be divided into two areas. The first one is a dynamic rotating mesh at the inner cylinder and the second one is a stationary mesh at the outer cylinder. There has to be defined an interface between this rotating and stationary area for exchanging the thermodynamic variables. These numerical investigations and the related comparisons to the experiment will be carried out in future works.

Nomenclature

B	nominal bearing width
e	eccentricity
H_0	nominal gap width
h	local gap width
p_o	relative pressure at the top axial end of the system
p_u	relative pressure at the bottom axial end of the system
Q_0	inner volumetric flow rate
Q_{in}	supply flow rate
Q_{out}	flow rate of outflowing fluid
R_1	radius inner cylinder (shaft)
R_2	radius outer cylinder (bushing)
Re	Reynolds number
u	circumferential speed
U_1	circumferential speed of the inner cylinder
α	ratio from applied volumetric flow rate to inner volumetric flow rate
Γ	relative bearing width
ψ	relative gap width
ε	relative eccentricity
ν	kinematic viscosity
φ	angle
φ_B	angle of the feedhole position
ω	angular velocity of the inner cylinder

References

1. M. Wollfarth, „Experimentelle Untersuchungen der Kavitationserosion im Gleitlager“ (1995)
2. M. Nobis, P. Stücke, M. Schmidt, C. Egbers, N. Scurtu, „Untersuchung der Zylinderspaltströmung unter Berücksichtigung der Geometrieformen realer Gleitlager“, 19. GALA conference, (2011)
3. G.I. Taylor, „Stability of a viscous liquid contained between two rotating cylinders“ (1923)
4. R.C. DiPrima, H.I. Swinney, , “Instabilities and Transistion in Flow Between Two Rotating Cylinders, in Hydrodynamic Instabilities and Transistion to Turbulence ” (1985)
5. P.M. Eagles, J.T. Stuart, R.C. DiPrima,: “The Effects of Eccentricity on Torque and Load in Taylor-Vortex Flow” (1978)
6. E.L. Koschmieder, “Taylor vortices between eccentric cylinders” (1976)
7. N. Scurtu, P. Stücke, C. Egbers, “Numerical and experimental study of the flow in an eccentric Couette-Taylor system with small gap” (2008)
8. M. Nobis, M. Schmidt, "Experimentelle und numerische Untersuchung der Schmierspaltströmung“ (2009)